Hindawi Publishing Corporation
Advances in Condensed Matter Physics
Volume 2013, Article ID 591787, 9 pages
http://dx.doi.org/10.1155/2013/591787

Hindawi

Research Article

Characterization of WO_3 Thin Films Grown on Silicon by HFMOD

Joel Díaz-Reyes,[1] Roberto Castillo-Ojeda,[2] Miguel Galván-Arellano,[3] and Orlando Zaca-Moran[1]

[1] *Centro de Investigación en Biotecnología Aplicada, Instituto Politécnico Nacional, Ex-Hacienda de San Juan Molino, 90700 Tepetitla, TLAX, Mexico*
[2] *Universidad Politécnica de Pachuca, Rancho Luna, Ex-Hacienda de Santa Bárbara, 43830 Zempoala, HGO, Mexico*
[3] *Departmento de Ingeniería Eléctrica, SEES, CINVESTAV-IPN. A. P. 14-740, 07000 México, DF, Mexico*

Correspondence should be addressed to Joel Díaz-Reyes; joel_diaz_reyes@hotmail.com

Received 27 May 2013; Accepted 30 July 2013

Academic Editor: S. J. Poon

Copyright © 2013 Joel Díaz-Reyes et al. This is an open access article distributed under the Creative Commons Attribution License, which permits unrestricted use, distribution, and reproduction in any medium, provided the original work is properly cited.

We studied the effect of annealing temperature on the physical properties of WO_3 thin films using different experimental techniques. WO_3 has been prepared by hot-filament metal oxide deposition (HFMOD). The films, chemical stoichiometry was determined by X-ray photoelectron spectroscopy (XPS). The monoclinic single-phase nature of the as-deposited films, structure was changed to triclinic structure by annealing them at higher temperatures than 400°C, which has been determined by the X-ray diffraction analysis. By Raman scattering is confirmed the change of crystalline phase, of monoclinic to triclinic, since that lattice vibrational modes of as-deposited WO_3 and annealed at 500°C present clearly differences. WO_3 band gap energy can be varied from 2.92 to 3.15 eV by annealing WO_3 from 0 to 500°C as was obtained by transmittance measurements. The photoluminescence response of the as-deposited film presents three radiative transitions observed at 2.85, 2.41, and 2.04 eV that could be associated with oxygen vacancies; the first one is shifted to higher energies as the annealing temperature is increased due to the change of crystalline phase of the WO_3.

1. Introduction

Transition metal oxides represent a large family of materials possessing various interesting properties, such as superconductivity, colossal magnetoresistance, and piezoelectricity. Among them, tungsten oxide is of great interest and has been investigated extensively for its distinctive properties. With outstanding electrochromic [1], photochromic [2], gas chromic [3], gas sensor [4], photocatalyst [5], and photoluminescence properties [6], as a result, tungsten oxide has been used to construct "smart-window," antiglare rear view mirrors for automobiles, nonemissive displays, optical recording devices, solid-state gas sensors, humidity and temperature sensors, biosensors, photonic crystals, and so forth.

WO_3 thin films can be prepared by various deposition techniques such as thermal evaporation [3, 7], spray pyrolysis [8], sputtering [9], pulsed laser ablation [4], sol-gel coating [10], and chemical vapour deposition [11]. The purpose of this work is to characterize the WO_3 layers deposited by hot filament metal oxide deposition (HFMOD) technique, which uses a metallic filament heated in a rarefied oxygen atmosphere [12]. The film is deposited on a substrate positioned near the filament, and the deposition rate is controlled by the filament temperature and the oxygen pressure, after they were annealed at a wide temperature range. This growth technique has some advantages compared to the conventional growth technique; easily implemented and it is not expensive. Both the thermochemistry of the process and the kinetics of film formation are currently under investigation. It is clear, however, that the film is formed from volatile Me_xO_y precursors, where Me is the metal, generated on the heated tungsten surface from reactions between oxygen and tungsten. The investigations so far carried out in our laboratory show that the films can be deposited with a good stoichiometric control, with relatively high deposition rates, presenting them a good adhesion to both metallic and dielectric substrates. Tests

on the electrochromic properties carried out on samples of WO_3 show that their optical efficiency is higher than that of WO_3 films obtained by the above-mentioned techniques. It is also important to remark that this technique differs from a deposition technique called hot filament chemical vapour deposition (HFCVD), which have been used to deposit siloxane [13] and diamond-like films [14], because the filament used here is not just a "catalyst" used to activate chemical species; it is also a reactant in the reaction. The characterization of the deposited material is carried out by XPS, X-ray diffraction, Raman spectroscopy, transmittance spectroscopy, and room-temperature photoluminescence.

2. Experimental Details

The WO_3 thin films were deposited by hot-filament metal oxide deposition (HFMOD) technique at atmospheric pressure on 100 oriented Si semi-insulating substrates at room temperature; the main growth system characteristics have been reported in the literature [12]. The thin films were annealed at different temperatures in the range from 100 to 500°C during 10 min in a nitrogen atmosphere. The chemical stoichiometry was determined by X-ray photoelectron spectroscopy (XPS) for the as-deposited film and annealed at 500°C. For the XPS analyses, a hemispherical spectrometer using the unmonochromatized Kα and X-ray line of aluminium was employed. Structural characterization of the samples was carried out by means of X-ray diffraction (XRD) in a Bruker D8 Discover diffractometer, with a parallel beam geometry and monochromator of Gobel mirror, Cu Kα radiation = 1.5406 Å, in the range of $20^{\circ} < 2\theta < 80^{\circ}$, by step of 0.02°. The XRD data were indexed using the program DICVOL04 with an absolute error of 0.03° in 2θ in calculates; all diffractograms were examined using the database ICDD PDF-(20-1324) [15]. Afterward, they were refine using the program POWDERX to determine the crystalline system and the parameters of unit cell. Raman scattering experiments were performed at room temperature using the 6328 Å line of He-Ne laser at normal incidence for excitation. The laser light was focused in a spot diameter of 6.0 μm on the sample using a 50x (numerical aperture 0.9) microscope objective. The nominal laser power used in these measurements was 20 mW. Scattered light was analyzed using a Dilor micro-Raman system (Lambram model); a holographic notch filter made by Kaiser Optical System, Inc. (model superNotch-Plus); a 256 × 1024-pixel CCD was used as detector and cooled to 140 K using liquid nitrogen and two interchangeable gratings (600 and 1800 g/mm). Typical spectrum acquisition time was limited to 60 s to minimize the sample heating effects. Absolute spectral feature position calibration to better than 0.5 cm^{-1} was performed using the observed position of Si which is shifted by 521.2 cm^{-1} from the excitation line. The transmittance measurements were performed using a Bruker Infrared Spectrometer Vertex 70. Room-temperature photoluminescence was taken with a solid state laser 325 nm with 60 mW as excitation source and a SCIENCETECH 9040 monochromator was used to perform the sweep of wavelength at room temperature in a cryostat CRYOGENICS.

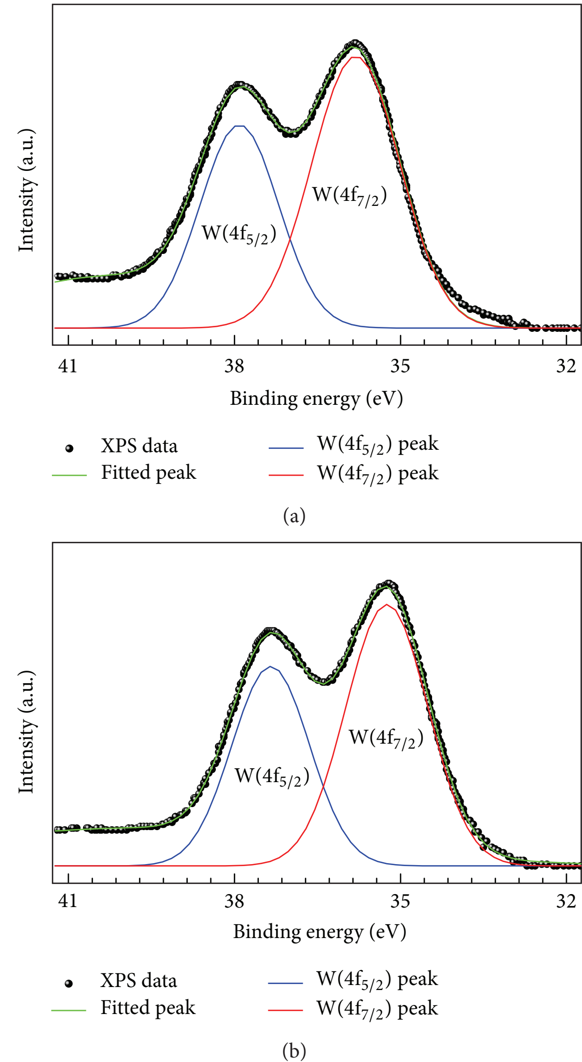

FIGURE 1: W(4f) core level spectra of WO_3 films: (a) as-deposited and (b) annealed at 500°C.

3. Results and Discussion

The elemental and chemical characterizations of the WO_3 films were performed by XPS on the as-deposited WO_3 sample and on the 500°C annealing one, which are shown in Figure 1. In the XPS spectrum (a) observes to $W(4f_{7/2})$ at 35.6 eV and $W(4f_{5/2})$ at 37.8 eV with a full width at half maximum (FWHM) of 1.75 eV. The area ratio of these two peaks is 0.75, which is supported by the spin-orbit splitting theory of 4f levels. Moreover, the structure was shifted by 5 eV towards higher energy relative to the metal state. It is thus clear that the main peaks in the XPS spectrum are attributed to the W^{6+} state on the surface [1], indicating that the as-deposited film is composed of stoichiometric WO_3. In stoichiometric WO_3, the six valence electrons of the tungsten atom are transferred into the oxygen p-like bands, which are thus completely filled. In this case, the tungsten 5d valence electrons have no part of their wavefunction near the tungsten atoms and the remaining electrons in the tungsten atom experience a

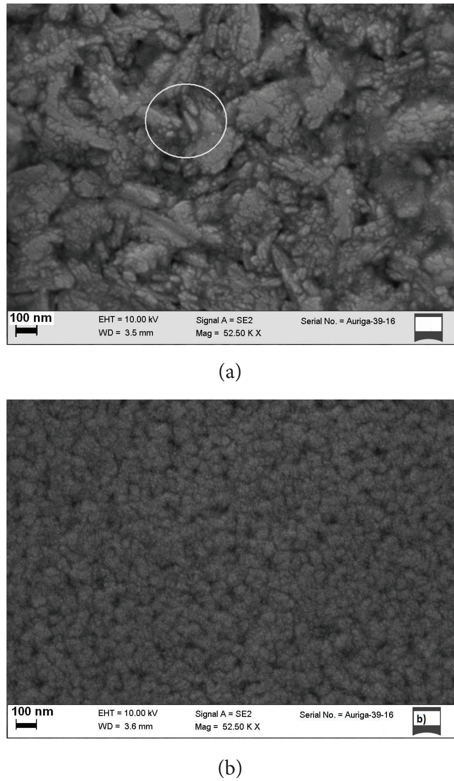

FIGURE 2: Typical surface morphology of WO_3 films grown by Hot-Filament Metal Oxide Deposition obtained by SEM to two annealing temperatures: (a) 0°C and (b) 500°C.

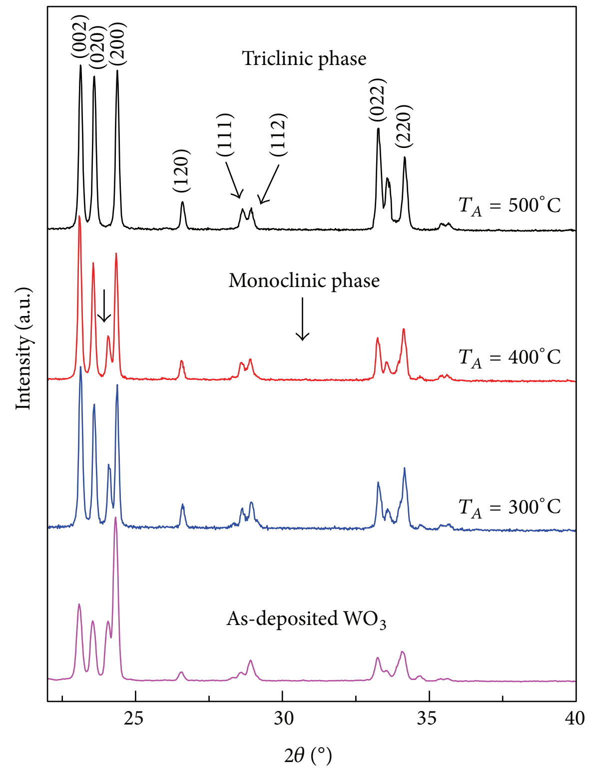

FIGURE 3: X-ray diffractogram of WO_3 films prepared on silicon substrates at 300 K and further annealed at different temperatures. The peak at $2\theta{\sim}24°$, related to the monoclinic phase, is indicated by an arrow.

stronger coulombic interaction with the nucleus than in the case of a tungsten atom in a metal, in which the screening of the nucleus has a component due to the 5d valence electrons. Therefore, the binding energy of the W(4f) level is larger in WO_3 than in metallic tungsten. If an oxygen vacancy exists, the electronic density near its adjacent W atom increases, the screening of its nucleus is higher, and, thus, the 4f level energy is expected to be at a lower binding energy [1]. For WO_3 film annealed at 500°C, the W(4f) peaks moved to a lower binding energy so that the $W(4f_{7/2})$ position was observed at 35.0 eV; see Figure 1(b). This behaviour can be due to the presence of water in our layers which evaporates during annealing. Then, this effect can be related to oxygen vacancies at this high annealing temperature and the formation of W^{5+}.

Figure 2 illustrates the surface morphology of typical as-grown WO_3 film and the 500°C annealing one obtained by SEM-EDS, which reveals the uniform roughness surface nature; besides the SEM-EDS measurements allow confirming the chemical composition of WO_3 layers grown by HFMOD. As is observed in the figure, there are some differences between the two morphologies; in the first one can see some nanostructures, which disappear with the heat process.

The X-ray diffraction pattern of as-deposited HFMOD WO_3 film on 100 silicon substrates is shown in Figure 3 that was measured from $2\theta = 20°$ to $40°$. It is observed from XRD pattern that WO_3 films deposited even at room temperature are of crystalline nature. This may be attributed to the fact that the crystalline silicon substrate facilitates the growth of crystalline WO_3 thin films, and their crystal lattice orientation is initiated on the silicon substrates at room temperature. By refinement of experimental X-ray data of as-deposited WO_3 using the software DICVOL04, the data finds that they are in good agreement with the monoclinic system reported in the ICDD PDF (20-1324) (WO_3) [15]. From this close agreement, it is confirmed that as-deposited hot-filament metal oxide deposition WO_3 films belong to the monoclinic crystal system. The X-ray pattern of as-deposited WO_3 film is described in the *P2l/n* whose lattice parameters were calculated using the software POWDERX, obtaining the following lattice parameters values: $a = 7.297$ Å, $b = 7.539$ Å, $c = 7.688$ Å, and $\beta = 90.91°$ and its unit lattice volume is about 422.88 $Å^3$, which are in agreement with the reported values [16]. Also, the formation of triplet peaks along *(00l)*, *(0k0)*, and *(h00)* growth orientations (where $h = k = l = 2$) shows that the films are grown along "*c*," "*b*," and "*a*" axes, respectively, confirming the columnar and textured nature of the films; see Figure 3. The intense and sharp peaks in X-ray diffraction pattern reveal the good crystallinity of the film and also confirm the stoichiometric nature of WO_3 films. The single-phase nature of the films also was confirmed from the presence of XRD peaks pertaining only to the WO_3 phase. With the increasing annealing temperature the intensity of the diffracted peaks becomes more intense and sharp that is indicative of a better crystallinity. The enhanced

preferential orientation after annealing at high temperatures may be due to the movement of deposited atoms along the surface of the substrate to reach the low-energy nucleation sites and to be preferentially deposited there itself. Furthermore, in Figure 3 are presented the XRD patterns of WO_3 samples annealed at different temperatures (300°C, 400°C, and 500°C). As has been reported in the literature, crystalline WO_3 presents a pseudocubic structure with a slight distortion of the cubic ReO_3-type lattice, being the most common crystalline structures at room temperature monoclinic and triclinic [17]. Due to the slight distortion of the lattice, the main reflection (200) of the ideal cubic cell splits into three reflections in the range 20–30° [18]: *(200)*, *(020)*, and *(002)* pseudo-cubic reflections. The differences between the X-ray patterns of the samples annealing at lower temperatures than 500°C should be attributed to the presence of some bulk defects that would mainly affect the *(002)* reflection peak. The XRD patterns obtained by the as-deposited samples and the annealed samples are very similar, except by the small peak sited at $2\theta\sim24^\circ$ that is indicated by the arrow in Figure 3 [19], which is associated with the monoclinic phase that disappears at higher annealing temperatures than 400°C, which is indicative of the WO_3 changes of dominant crystalline phase with the annealed ones, at triclinic phase [19]. Besides, as has been reported in the literature, it should follow the change in the diffraction peak sited at about $2\theta\sim34^\circ$ [19] that allows making a clear attribution of the crystalline structure of the different samples, in this study the peak observed at about 34° change appreciably which should allow distinguishing clearly between monoclinic and triclinic structures. Using the same software POWDERX, the data were obtained the lattice parameters of the triclinic structure whose values are $a = 7.31261$ Å, $b = 7.52521$ Å, $c = 68937$ Å, $\alpha = 88.85^\circ$, $\beta = 90.91^\circ$, and $\gamma = 90.94^\circ$ and its unit lattice volume is about 422.94 Å^3. It is interesting to notice the evolution of their maximum intensity and their full width at half maximum (FWHM) with the annealing temperature of these three main peaks. Experimental spectra show that the relating intensity of the peak corresponding to *(002)* reflection (at 23.08°) is higher than the other two up to 400°C-annealing, reaching a similar value after 500°C annealing; see Figure 3. A similar behaviour is reflected by the evolution of FWHM of *(002)* reflection that is shown in Figure 4, as it only approaches the values of the other two peaks after a 400°C-annealing. Figure 4 also included the peak associated with monoclinic phase to follow its behaviour with the annealing temperature and its disappearance. This behaviour indicates that the thin films improve their crystalline quality with the annealing processes.

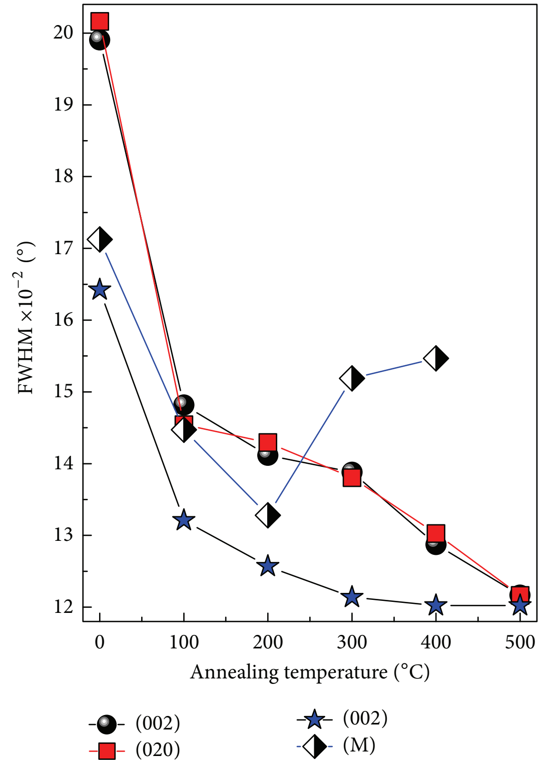

Figure 4: Evolution of FWHM of the four main XRD reflections as function of the annealing temperature.

Raman spectra of as-deposited and annealed WO_3 films are shown in Figure 5, which were measured at the range from 1000 to 50 cm^{-1}. The numbers to the right of graphs indicate that increasing temperature increases Raman intensity. The Raman spectroscopy can give a clearer evidence of the phase changes and allows following the different steps of the transformation by analysing the evolution of lowest frequency peaks (up to 200 cm^{-1}) of the Raman spectra [19]. These peaks correspond to lattice modes of vibrational natural that are noticeably affected by the transitions between the low symmetry phases of WO_3, which involve mainly collective rotations of the basic $[WO_6]$ octahedral units. Most vibrational peaks below 200 cm^{-1} in the WO_3 Raman spectrum are attributed to lattice modes, whereas the mid- and high-frequency regions correspond to deformation and stretching modes, respectively. As can be observed from Figure 5 there is no feature with highest frequency to the peak of 801 (811) cm^{-1} in the Raman spectrum of the crystalline WO_3 film as-deposited (annealed), which is a good evidence, since WO_3 crystal does not have any double bond [20, 21] and this is observed above that frequency. The Raman spectrum of as-deposited WO_3 presents four main vibrational bands in the range of 1000–200 cm^{-1} observed at 801, 710, 322, and 262 cm^{-1}. The intense peaks at 801 and 710 cm^{-1} are typical Raman peaks of crystalline WO_3 (m-phase), which correspond to the stretching vibrations of the bridging oxygen [22, 23], and these are assigned to W–O stretching (ν), W–O bending (δ), and O–W–O deformation (γ) modes, respectively [24, 25]. This great number of active Raman modes is due to the distortion of the ReO_3-type structure in real monoclinic situation, as the group theory shows that this structure should only have two active modes [19]. The sharp peaks at 262 and 322 cm^{-1} are assigned to the bending vibration δ(O–W–O) [24, 26]. The Raman peak at 262 cm^{-1} is intense enough, which means that a great fraction of monocrystalline phase is present in the as-deposited films. The peaks observed at 801, 710, and 262 cm^{-1} are very intense, and these are typical

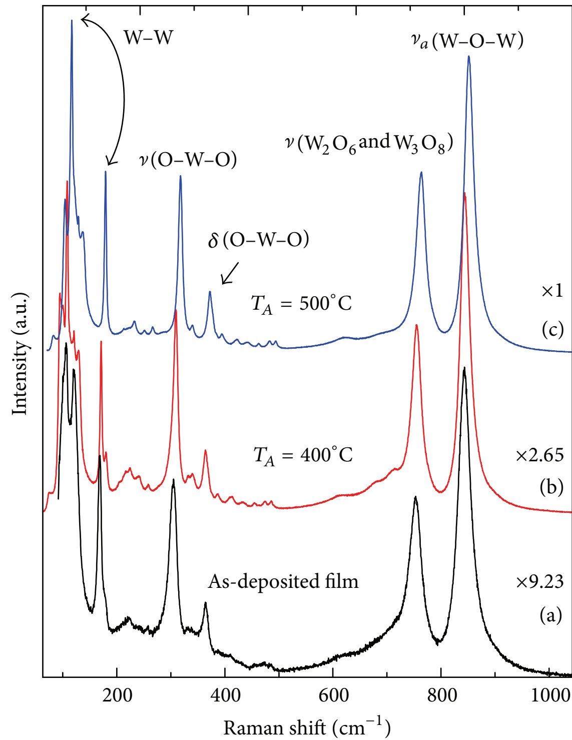

Figure 5: Raman spectra of WO_3 thin films annealed at different temperatures.

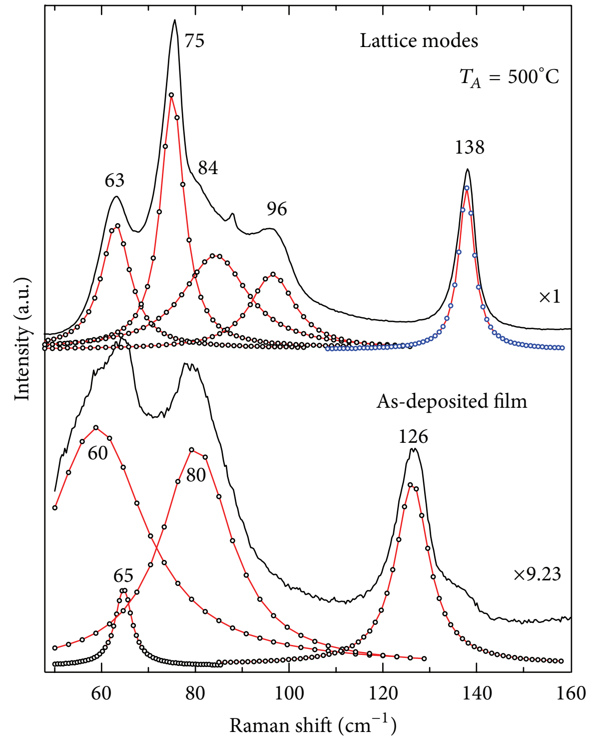

Figure 6: Raman spectra of two WO_3 thin films at low frequencies: as-deposited and annealed at 500°C.

modes of the crystalline WO_3 (monoclinic phase). All these peaks are in good agreement with what has been published on WO_3 deposited by conventional techniques. The Raman spectra of the samples annealed at 400 and 500°C are shown in Figure 5. Before and after annealing the WO_3 films show similar Raman spectra for the range 1000–200 cm^{-1} [27]. Variations of the intensity between the Raman spectra are found in all frequency ranges; furthermore, the Raman spectrum of WO_3 sample annealed at 500°C is slightly displaced to blue possibility due to the increment of oxygen vacancies and the phase change. All the noise background from the underlying silicon slide in the spectra decreases after annealing at 300°C; that is, the I_R/I_N ratio of Raman intensity (I_R) and noisy signal intensity (I_N) increased after annealing.

Figure 6 illustrates the Raman spectra in the range 160–50 cm^{-1} of two samples: eliminate as-deposited WO_3 and 500°C-WO_3. Figure 6(a) shows the Raman spectrum for the as-deposited sample, which presents four peaks observed at 126, 84, 65, and 60 cm^{-1}. These are typical characteristic peaks of the monoclinic crystalline phase at low frequencies that were obtained by deconvolution using Lorentzian curves and allowed finding the peaks frequencies that are associated with lattice modes [26, 28]. Similar vibration modes were obtained by Raman theories and are in agreement with the reported results [23]. As is observed in Figure 6(b), the Raman spectrum of 500°C-WO_3 shows that its peaks are enhanced by the annealing. By the way, as the vibrational modes at low frequencies are associated with the lattice modes, as is observed in Figure 6(a), the main vibrational bands present in the Raman spectrum of as-deposited WO_3 film are different from the vibrational modes present in the Raman spectra of the films annealed at higher temperatures than 400°C, which is indicative of the annealing WO_3 films change of crystalline phase with the heat treatments, from monoclinic to triclinic phase. Table 1 presents all the modes frequencies observed in the present study. All the vibrational modes observed at frequencies higher that 160 cm^{-1} in the Raman spectra of annealed samples are slightly shifted toward the blue. Gazzoli et al. [29] indicated that the vibrational bands positions in Raman spectrum depend on the tungsten content: a higher tungsten content, the higher the frequency at which the bands appear in the Raman spectrum and the removal of water molecules causes a shift of the Raman bands at higher frequency, which was confirmed by XPS studies. There is a difference in our ex-situ Raman spectra before and after heat treatment. The peak at 801 cm^{-1} shifts slightly to higher frequency (811 cm^{-1}) after annealing. Due to the above statements, the 811 cm^{-1} peak should indicate that the WO_3 film contains more oxygen deficiency and the 801 cm^{-1} one should indicate more moisture on the film before annealing. Since it is an ex-situ measurement, even if we remove the surface water molecules of the films they can be partly absorbed on surface again during the experiment after annealing. Hence we deduced that the Raman shift comes from the internal structure or phase of the film, not from the surface of the film.

All the above facts support the hypothesis of an open (or porous) structure of the films with many inner empty spaces and intergrain boundaries. This means that comparably small

Table 1: Raman bands for monoclinic and triclinic phases of WO_3 and their assignments.

Monoclinic wavenumber (cm^{-1})	Triclinic wavenumber (cm^{-1})	Raman groups and assignments
60	63	W–W
65	75	W–W
80	84	W–W
—	96	W–W
126	138	W–W
269	276	ν(O–W–O)
322	331	δ(O–W–O)
710	721	$\nu(W_2O_6$ & $W_3O_8)$
801	812	ν(W–O–W)

amounts of water were absorbed in the films. The results suggest that the formation of porous films is due to gas-phase reactions in the plasma, leading to a homogeneous nucleation of oxide particles on the substrate. Clearly the prepared films were not a typical crystalline WO_3 (monoclinic phase or m-phase) structure. In addition probably an increase of compressive residual stress of the film due to annealing causes Raman shift to higher wavenumbers. This phenomenon has also been observed in IrO_2 films [30], ZrO_2 films [31], and on the GaAs-SiO_2 interface [32]. Considering the residual stress and the Raman peak position before and after annealing, it can be concluded that the Raman peak position shifts to higher wavenumbers with the increase of compressive stress and it shifts to lower wavenumbers with the increase of tensile stress. To obtain a quantitative measurement of the residual stress of the WO_3 films, more detailed work is needed.

The samples used for transmission measurements were deposited on silicon substrates of 100 μm of thickness, which were obtained by chemical etching. The transmittance spectra in the visible and infrared range are recorded for the WO_3 thin films before and after annealing at different temperatures in the energy range 1.5–3.1 eV. The effect of annealing temperature on the optical properties including percentage of transmittance (% of T) and energy band gap (E_g) is studied in detail. Figure 7 shows the transmission spectra of WO_3 films that are prepared at room temperature on silicon and further heat treated (annealed) in the range 100–500°C. The observed transmittance of the as-deposited film in the visible range varies from about 1 up to nearly 4% (without considering the substrate contribution). The sharp reduction in the transmittance spectrum at the energy of 3.15 eV is due to the fundamental absorption edge that was also reported previously [1]. The as-deposited tungsten oxide films were transparent, with no observable blue colouration under our experimental conditions. The transmittance of the WO_3 film annealed at 500°C is increased by about 10%, as can be seen in Figure 7. The increase in transparency of the films with increased annealing temperature in air environment may be due to the formation of more oxygen-ion vacancies in the films and crystalline phase change as has been observed by X-ray dispersion and Raman scattering; the film changes to a nonstoichiometric composition, as could be seen from

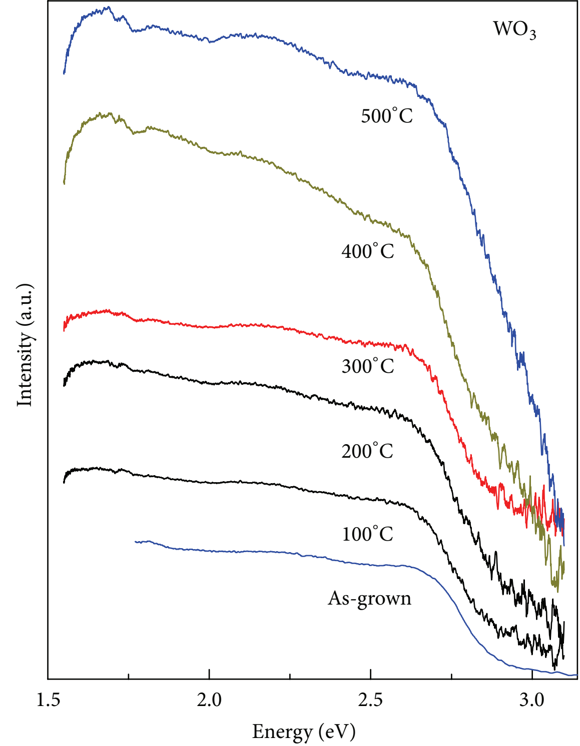

Figure 7: Optical transmittance of the WO_3 thin films annealed at different temperatures.

the change in colour of the film due to the excellent electrochromic nature. This causes the slight increase in energy band gap. It confirms that the improvement in crystallinity of the films increases with increasing annealing temperature; see Figure 7. It is observed from the transmittance spectra that the absorption edge is also slightly shifted towards the higher energy region for the films annealed at higher temperatures, owing to preferred colouration effect on the films. The colour of the films also changes with the annealing temperatures, due to the excellent electrochromic nature.

The intrinsic absorption edge of the films can be evaluated and discussed in terms of the indirect interband transition. The optical band gap (E_g) was evaluated by the absorption coefficient α using the standard relation: $(\alpha h\nu)^{1/2} = A(h\nu - E_g)$ is expected to show a linear behaviour in the higher energy region, which should correspond to a strong absorption near the absorption edge. Extrapolating the linear portion of this straight line to zero absorption edge gives the optical energy band gap, E_g, of the films. The absorption coefficient α for a film of thickness d and reflectance R was determined near the absorption edge using the simple relation $\alpha = \ln\{(1-R)^2/T + [((1-R^2)/2T)^2 + R^2]^{1/2}\}/d$, where multiple reflections are taken into account, but interference is neglected, and d is the film thickness. Actually a transmission interference pattern could be observed in most samples and was used to obtain an accurate value for thickness d. The optical band gap for the as-deposited WO_3 is calculated to be about 2.92 eV; the polycrystalline structure of

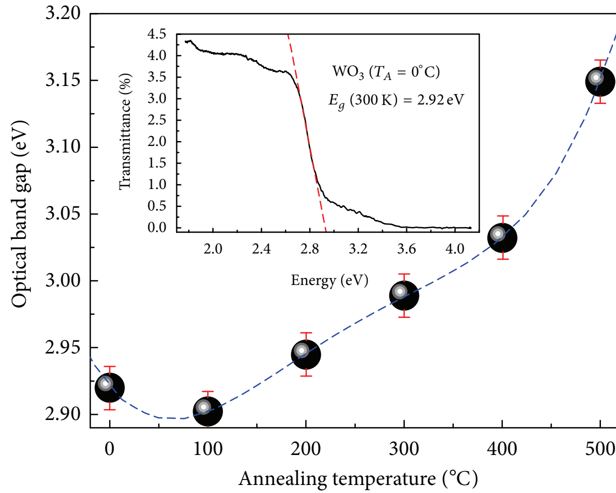

FIGURE 8: Optical band gap energy of the WO_3 thin films as-deposited and annealed at different temperatures. The inset shows absorption edge that allows calculating the band gap for the as-deposited sample.

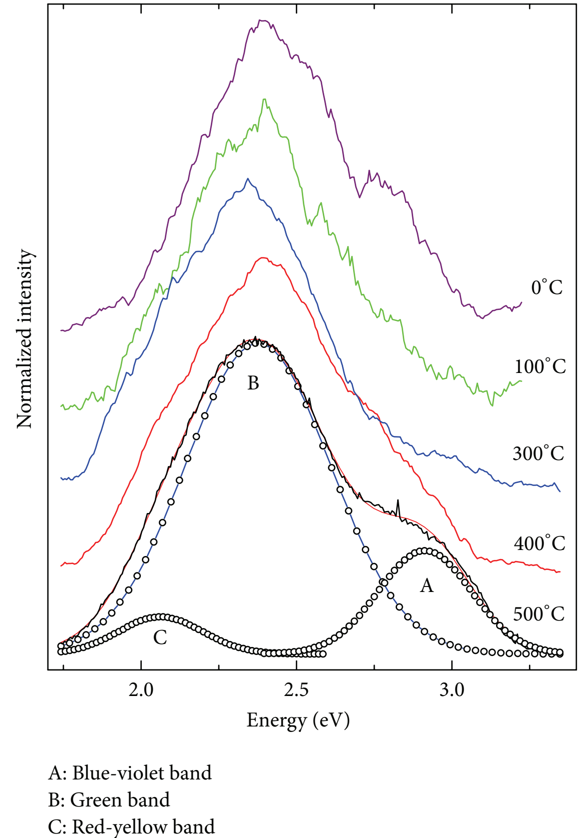

A: Blue-violet band
B: Green band
C: Red-yellow band

FIGURE 9: Room-temperature photoluminescence of the as-deposited and annealed WO_3 thin films at different temperatures.

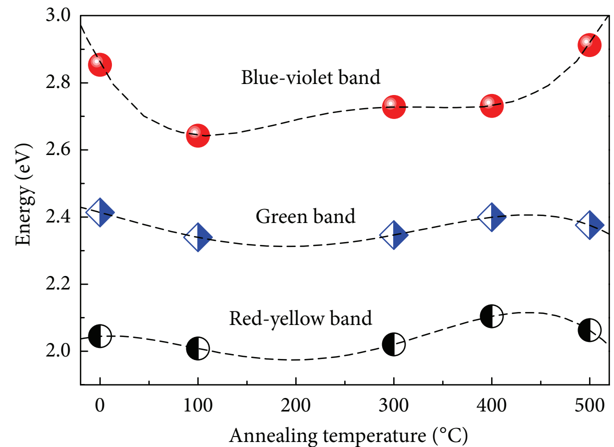

FIGURE 10: It shows the energetic behaviour of the three bands existent in the 300 K PL spectra.

the as-deposited WO_3 could cause E_g to be bigger than 2.7 eV that corresponds to pure WO_3 indirect band gap in bulk. For the sample annealed at 100°C, the optical band gap decreased slightly by about 0.02 eV, which can be related to condensation of the films. However, the optical band gap of the WO_3 annealed at the range from 200 to 500°C is increased up to 3.15 eV due to recrystallization of the film. The reasons for which E_g becomes bigger than 2.7 eV is the formation of oxygen vacancies at hese temperatures and the change of crystalline phase, as can be seen in Figure 8 [33, 34]. It is worth noting that has reported in the literature that for WO_3 films deposited by evaporation has found $2.7 < E_g < 3.5$ eV [1]. The inset in the figure shows the absorption edge of the as-deposited WO_3, which allows calculating the band gap, that is, 2.92 eV. Besides, the graph contains the error bars that were calculated with precision of 5%.

Figure 9 illustrates the 300 K photoluminescence of the as-deposited sample; it presents three radiative transitions, labelled A, B, and C and sited at 2.85, 2.41, and 2.04 eV that might be associated with oxygen vacancies, although band B is more intense for the investigated annealing temperature range. As can be seen in Figure 10, the band labelled A is associated with blue-violet band and changes its radiative energy in a wide range, $\Delta E = 269.6$ meV. The same occurs with bands B and C oscillating in a band of 74 and 96 meV as the annealing temperature is increased. Figure 11 shows the dependence of the radiative bands, intensity versus annealing temperature; as is observed they tend to increase as the annealing temperature is increased presenting a minimum around 100°C. These results could be related to oxygen vacancies generated by the annealing ones and crystalline phase change.

4. Conclusions

In this work we have investigated in detail the effect of annealing temperature on structural and optical hot-filament metal oxide deposition WO_3 films. X-ray diffraction analysis clearly shows the formation of predominant triplet peaks along *(002)*, *(020)*, and *(200)* growth orientations, which exhibit the monoclinic, single-phase growth nature of the films, for the as-deposited and annealed samples. The transformation of crystalline phase of the films deposited on silicon substrates was observed when one increases

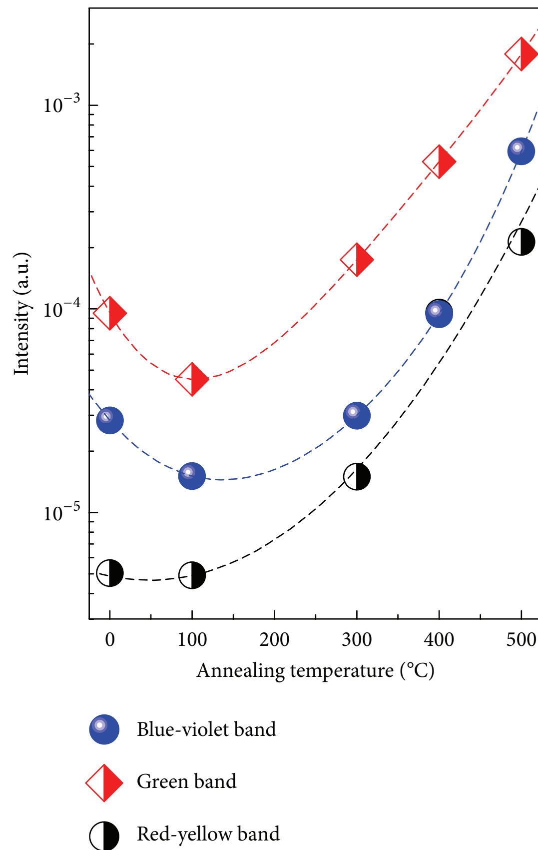

FIGURE 11: Intensity versus annealing temperature for three bands that presents the 300 K PL spectra. The dash line is a figure-of-merit to follow the experimental points.

the annealing temperature above 400°C, monoclinic to triclinic phase. The better aligned and highly oriented growth peaks enumerate the stoichiometric nature of the films. The highly transparent nature of the films has been observed from the optical transmittance spectra. The increase in transmittance with increasing annealing temperatures reveals the formation of oxygen vacancies in the films. The slight widening in the evaluated optical energy band gap values towards the increasing annealing temperature may be due to the optical band filling effect that reveals the crystallization of the films. One believes that these preliminary characteristic observations on the hot-filament metal oxide deposition WO_3 films will be helpful to explore the device performance of the films for electrochromic and smart window applications.

References

[1] C. G. Granqvist, *Handbook of Electrochromic Materials*, Elsevier, Amsterdam, The Netherlands, 1995.

[2] C. O. Avellaneda and L. O. S. Bulhoes, "Photochromic properties of WO_3 and WO_3:X (X = Ti, Nb, Ta and Zr) thin films," *Solid State Ionics*, vol. 165, no. 1–4, pp. 117–121, 2003.

[3] S. H. Lee, H. M. Cheong, P. Liu et al., "Gasochromic mechanism in a-WO_3 thin films based on Raman spectroscopic studies," *Journal of Applied Physics*, vol. 88, no. 5, pp. 3076–3078, 2000.

[4] E. György, G. Socol, I. N. Mihailescu, C. Ducu, and S. Ciuca, "Structural and optical characterization of WO_3 thin films for gas sensor applications," *Journal of Applied Physics*, vol. 97, no. 9, Article ID 093527, 5 pages, 2005.

[5] M. A. Gondal, A. Hameed, Z. H. Yamani, and A. Suwaiyan, "Laser induced photo-catalytic oxidation/splitting of water over α-Fe_2O_3, WO_3, TiO_2 and NiO catalysts: Activity comparison," *Chemical Physics Letters*, vol. 385, no. 1-2, pp. 111–115, 2004.

[6] M. Feng, A. L. Pan, H. R. Zhang et al., "Strong photoluminescence of nanostructured crystalline tungsten oxide thin films," *Applied Physics Letters*, vol. 86, no. 14, Article ID 141901, 3 pages, 2005.

[7] R. Azimirad, O. Akhavan, and A. Z. Moshfegh, "Influence of coloring voltage and thickness on electrochromical properties of e-beam eaporated WO_3 thin films," *Journal of the Electrochemical Society*, vol. 153, no. 2, pp. E11–E16, 2006.

[8] J. Hao, S. A. Studenikin, and M. Cocivera, "Transient photoconductivity properties of tungsten oxide thin films prepared by spray pyrolysis," *Journal of Applied Physics*, vol. 90, no. 10, pp. 5064–5069, 2001.

[9] Y. Takeda, N. Kato, T. Fukano, A. Takeichi, T. Motohiro, and S. Kawai, "WO_3/metal thin-film bllayered structures as optical recording materials," *Journal of Applied Physics*, vol. 96, no. 5, pp. 2417–2422, 2004.

[10] G. Garcia-Belmonte, P. R. Bueno, F. Fabregat-Santiago, and J. Bisquert, "Relaxation processes in the coloration of amorphous WO_3 thin films studied by combined impedance and electro-optical measurements," *Journal of Applied Physics*, vol. 96, no. 1, pp. 853–859, 2004.

[11] M. Seman and C. A. Wolden, "Investigation of the role of plasma conditions on the deposition rate and electrochromic performance of tungsten oxide thin films," *Journal of Vacuum Science and Technology A*, vol. 21, no. 6, pp. 1927–1933, 2003.

[12] J. Díaz-Reyes, V. Dorantes-García, A. Pérez-Benítez, and J. A. Balderas-López, "Obtaining of films of tungsten trioxide (WO_3) by resistive heating of a tungsten filament," *Superficies y Vacío*, vol. 21, no. 2, pp. 12–17, 2008.

[13] H. G. Pryce Lewis, T. B. Casserly, and K. K. Gleason, "Hot-filament chemical vapor deposition of organosilicon thin films from hexamethylcyclotrisiloxane and octamethylcyclotetrasiloxane," *Journal of the Electrochemical Society*, vol. 148, no. 12, pp. f212–f220, 2001.

[14] C. Li, K. C. Feng, Y. J. Fei, H. T. Yuan, Y. Y. Xiong, and K. Feng, "The influence of C_{60} as intermediate on the diamond nucleation on copper substrate in HFCVD," *Applied Surface Science*, vol. 207, no. 1-4, pp. 169–175, 2003.

[15] PDF-ICDD-Power Diffraction File, International Centre for Diffraction Data, USA, 2009.

[16] R. Sivakumar, R. Gopalakrishnan, M. Jayachandran, and C. Sanjeeviraja, "Preparation and characterization of electron beam evaporated WO_3 thin films," *Optical Materials*, vol. 29, no. 6, pp. 679–687, 2007.

[17] S. Santucci, C. Cantalini, M. Crivellari, L. Lozzi, L. Ottaviano, and M. Passacantando, "X-ray photoemission spectroscopy and scanning tunneling spectroscopy study on the thermal stability of WO_3 thin films," *Journal of Vacuum Science and Technology A*, vol. 18, no. 4 I, pp. 1077–1082, 2000.

[18] J. G. Allpress, R. J. D. Tilley, and M. J. Sienko, "Examination of substoichiometric WO_{3-x} crystals by electron microscopy," *Journal of Solid State Chemistry*, vol. 3, no. 3, pp. 440–451, 1971.

[19] E. Cazzanelli, C. Vinegoni, G. Mariotto, A. Kuzmin, and J. Purans, "Low-temperature polymorphism in tungsten trioxide

powders and its dependence on mechanical treatments," *Journal of Solid State Chemistry*, vol. 143, no. 1, pp. 24–32, 1999.

[20] M. F. Daniel, B. Desbat, J. C. Lassegues, and R. Garie, "Infrared and Raman spectroscopies of rf sputtered tungsten oxide films," *Journal of Solid State Chemistry*, vol. 73, no. 1, pp. 127–139, 1988.

[21] H. N. Cui, *Preparation and characterization of optical multilayered coatings for smart windows applications [Doctoral Thesis]*, University of Minho, 2005.

[22] P. Tägtström and U. Jansson, "Chemical vapour deposition of epitaxial WO_3 films," *Thin Solid Films*, vol. 352, no. 1-2, pp. 107–113, 1999.

[23] G. A. de Wijs and R. A. de Groot, "Amorphous WO_3: a first-principles approach," *Electrochimica Acta*, vol. 46, no. 13-14, pp. 1989–1993, 2001.

[24] M. F. Daniel, B. Desbat, J. C. Lassegues, B. Gerand, and M. Figlarz, "Infrared and Raman study of WO_3 tungsten trioxides and WO_3, $_xH_2O$ tungsten trioxide tydrates," *Journal of Solid State Chemistry*, vol. 67, no. 2, pp. 235–247, 1987.

[25] E. Salje, "Crystal physics, diffraction, theoretical and general crystallography," *Acta Crystallographica Section A*, vol. 31, no. 3, pp. 360–363, 1975.

[26] A. Rougier, F. Portemer, A. Quédé, and M. El Marssi, "Characterization of pulsed laser deposited WO_3 thin films for electrochromic devices," *Applied Surface Science*, vol. 153, no. 1, pp. 1–9, 1999.

[27] J. V. Gabrusenoks, P. D. Cikmach, A. R. Lusis, J. J. Kleperis, and G. M. Ramans, "Electrochromic colour centres in amorphous tungsten trioxide thin films," *Solid State Ionics*, vol. 14, no. 1, pp. 25–30, 1984.

[28] M. Regragui, M. Addou, A. Outzourhit et al., "Preparation and characterization of pyrolytic spray deposited electrochromic tungsten trioxide films," *Thin Solid Films*, vol. 358, no. 1, pp. 40–45, 2000.

[29] D. Gazzoli, M. Valigi, R. Dragone, A. Marucci, and G. Mattei, "Characterization of the zirconia-supported tungsten oxide system by laser Raman and diffuse reflectance spectroscopies," *Journal of Physical Chemistry B*, vol. 101, no. 51, pp. 11129–11135, 1997.

[30] P. C. Liao, C. S. Chen, W. S. Ho, Y. S. Huang, and K. K. Tiong, "Characterization of IrO_2 thin films by Raman spectroscopy," *Thin Solid Films*, vol. 301, no. 1-2, pp. 7–11, 1997.

[31] A. Portinha, V. Teixeira, J. Carneiro, M. F. Costa, N. P. Barradas, and A. D. Sequeira, "Stabilization of ZrO_2 PVD coatings with Gd_2O_3," *Surface and Coatings Technology*, vol. 188-189, no. 1–3, pp. 107–115, 2004.

[32] A. B. M. Harun-ur Rashid, M. Kishi, and T. Katoda, "Raman spectroscopic analysis of stress on GaAs-SiO_2 interface and the effect of stress on tin diffusion in GaAs," *Journal of Applied Physics*, vol. 80, no. 6, pp. 3540–3545, 1996.

[33] S. Z. Karazhanov, Y. Zhang, A. Mascarenhas, S. Deb, and L.-W. Wang, "Oxygen vacancy in cubic WO_3 studied by first-principles pseudopotential calculation," *Solid State Ionics*, vol. 165, no. 1-4, pp. 43–49, 2003.

[34] R. Chatten, A. V. Chadwick, A. Rougier, and P. J. D. Lindan, "The oxygen vacancy in crystal phases of WO_3," *Journal of Physical Chemistry B*, vol. 109, no. 8, pp. 3146–3156, 2005.

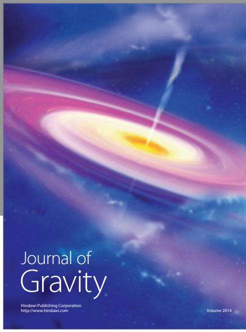
Journal of
Gravity

Journal of
Photonics

The Scientific
World Journal

Journal of
Soft Matter
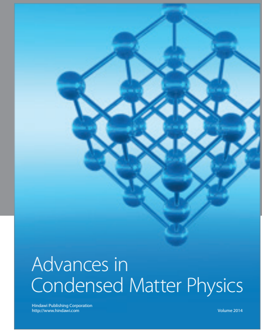
Advances in
Condensed Matter Physics

Journal of
Fluids

Hindawi
Submit your manuscripts at
http://www.hindawi.com
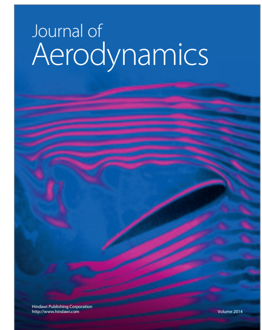
Journal of
Aerodynamics

International Journal of
Statistical Mechanics
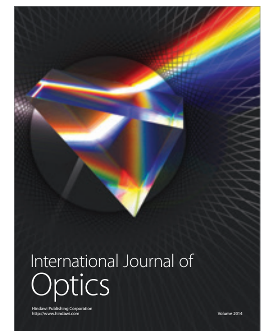
International Journal of
Optics
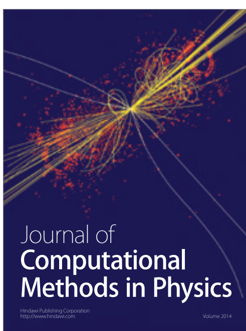
Journal of
Computational
Methods in Physics
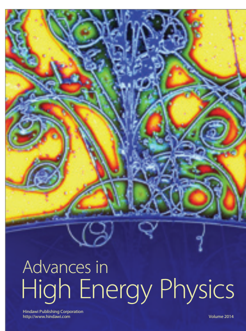
Advances in
High Energy Physics

Journal of
Thermodynamics
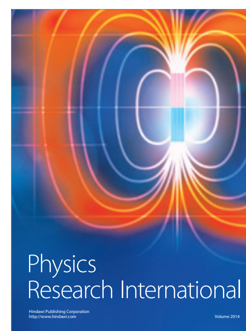
Physics
Research International
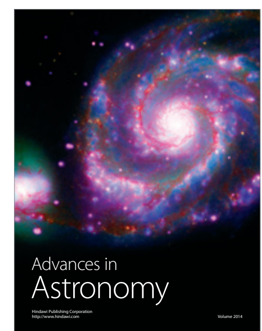
Advances in
Astronomy
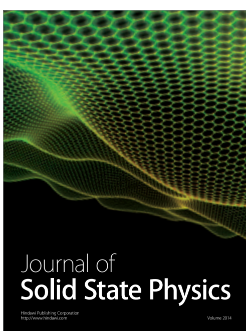
Journal of
Solid State Physics

Journal of
Astrophysics

International Journal of
Superconductivity
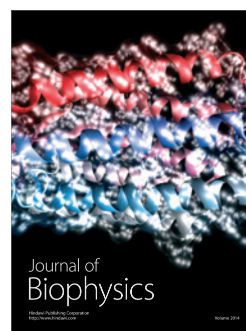
Journal of
Biophysics
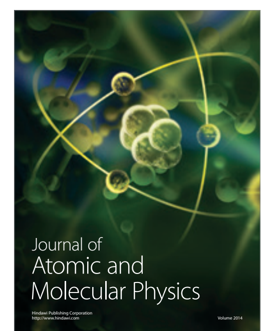
Journal of
Atomic and
Molecular Physics